

*J. Nano- Electron. Phys.*  
3 (2011) No1, P.17-25

© 2011 SumDU  
(Sumy State University)

PACS numbers: 61.05.cp, 81.05.Ea

## THE STUDY OF MICROSTRUCTURE OF III-V POLAR ON NON-POLAR HETEROSTRUCTURES BY HRXRD

*Ravi Kumar\**, *Tapas Ganguli*, *Vijay Chouhan*, *V.K. Dixit*

Raja Ramanna Centre for Advanced Technology,  
452013, Indore, India  
\* E-mail: [ravi@rrcat.gov.in](mailto:ravi@rrcat.gov.in)

*In this article, we report on the detailed high resolution x-ray diffraction data analysis of three GaAs films deposited by metal organic vapour phase epitaxy on Si substrates. In the GaAs/Si films the effect of anti phase domains is seen by the selective broadening of (002) and (006) reflections. Further as the (006) reflection is a very weak reflection, such films cannot be analyzed by conventional Williamson-Hall plots using (002), (004) and (006) reflections. We find that using (111), (333) and (444) reflections it is possible to use the standard Williamson-Hall analysis and extract parameters related to the microstructure of the films. We have also carried out the analysis to determine the tilt and twist between the mosaic blocks after correcting for the effects of the finite lateral coherence length.*

**Keywords:** HRXRD, GaAs/Si, ANTIPHASE DOMAINS, MICROSTRUCTURE, MISMATCHED EPITAXY.

(Received 04 February 2011, in final form 21 March 2011)

### 1. INTRODUCTION

High Resolution X-Ray Diffraction (HRXRD) is a powerful non-destructive tool for the analysis of the microstructure of epitaxial systems. There have been several works in recent times, where HRXRD has been used for the understanding of the microstructure of heteroepitaxial layers, like in GaN [1-3], InN [4, 5], ZnO [6], etc.

Williamson Hall (W-H) plots have been used for the analysis of both epitaxial layers and polycrystalline systems for a long time [7]. There has been a large body of work where W-H plots have been used for the analysis of the Lateral Coherence Length (LCL), tilt, vertical coherence lengths and microstrain in epitaxial and oriented polycrystalline films with wurtzite structure, e.g. epitaxial GaN and AlGaIn [3], epitaxial InN [4, 5], polycrystalline GaN [8] and polycrystalline ZnO [9]. In all these analysis, the authors have used the reflections from planes perpendicular to the growth direction namely, (0002) (0004) and (0006). There are very few reports on the application W-H plots for the analysis of the microstructure of epitaxial zinc-blende structures deposited on mismatched substrates. In one of the detailed reports, Neumann et al. have used the W-H plots to analyze GaAs/Si system [10]. This system has another complication which is related to the growth of the polar material (namely GaAs) on non-polar Si substrates resulting on the generation of Anti phase domains (APDs). The presence of APDs has been seen in several systems including metallic alloys and is known to broaden selective reflections [10, 11]. In the case of the zinc-

blende systems, the presence of APDs result in the broadening of reflections like (002) and (006) where the expression for the scattering amplitude has the difference of the contributions from the group III and group V atoms [10]. Additionally the (006) reflection is a weak reflection in zinc-blende systems. Further in the case of lattice mismatched zinc-blende epitaxial layers like GaP/GaAs [20], GaSb/GaAs [16], InAs/GaAs etc. [17] which are of contemporary research interest for optoelectronic devices and where APDs are not an issue, the (006) reflection is a very weak, thereby resulting in errors in the determination of the widths. Thus, the W-H analysis using the (002), (004) and (006) reflections cannot be used. In this work, we show that a set of planes parallel to the (111) plane can be alternatively used for the W-H analysis, thereby enabling us the study the microstructure of the zinc-blende layers with very weak (006) reflections.

Following the work of Srikant et al. [12], there has been a lot of work related to the analysis of tilt and twist between the mosaic blocks in lattice mismatched systems for wurtzite systems [13]. However, to the best of our knowledge, there has been no attempt to analyze the tilt and twist between the mosaic blocks in zinc-blende systems. We have carried out a detailed analysis of the tilt and twist using the method proposed by Lee et al. [3] after carrying out LCL corrections.

Although we have looked only at samples of GaAs/Si, the analysis procedure is very general and can be used for any zinc-blende system with APDs like GaP/Si [14,19], GaSb/Si [15] or without APDs like GaSb/GaAs [16]. Thus the proposed methods have a broad range of applicability.

## 2. EXPERIMENTAL AND ANALYSIS TECHNIQUES

HRXRD measurements have been carried out on a Panalytical X'Pert PRO MRD system. The measurements were made in either the skew-symmetric or the symmetric geometry for different planes (Planes of the type  $(00l)$  were analyzed in the symmetric geometry and of the type  $(h, k, l)$  with  $h$  and/or  $k \neq 0$ , were analyzed in the skew-symmetric geometry). A hybrid monochromator (Goebel's mirror with a four-bounce crystal monochromator), which gives  $\text{CuK}\alpha_1$  (wavelength = 1.54056 Å) output with a beam divergence of  $\sim 20$  arcsecs, was used for making the measurements. For GaAs/Si samples a three-bounce collimator (also referred to as triple-axis attachment) is placed in front of the detector to ensure an acceptance angle of  $\sim 12$  arcsecs. The  $\omega$  - scans in both the symmetric and skew-symmetric geometries have been recorded in the triple-axis geometry for the GaAs/Si samples.

The recorded data is converted in  $q$  - space for further analysis using the following relations:

$$q_x = \left(\frac{1}{\lambda}\right) [\cos \omega - \cos (2\theta - \omega)] \quad (1)$$

$$q_z = \left(\frac{1}{\lambda}\right) [\sin \omega + \sin (2\theta - \omega)] \quad (2)$$

where,  $\lambda$  is the wavelength of the incident X-ray,  $\omega$  is the angle the sample makes with the sample surface and the  $2\theta$  is angle of deviation of the diffracted beam from the incident beam direction.

The  $\omega$  - scan widths are generally represented by Gaussian line shape profile with two main broadening mechanisms namely: finite LCLs and angle misorientation between the mosaic blocks. The LCL is an average of a large distribution of random sizes of the mosaic blocks. Similarly the angle between the mosaic blocks due to tilts and twists are also from a random distribution of dislocations thereby resulting in a Gaussian broadening. In such a case the total width of the  $\omega$  - scans can be written as:

$$\left(\Delta q_{obs}(\omega)\right)^2 = \left(\Delta q_{(001)LCL}\right)^2 + (\alpha_{tilt} \cdot q)^2 \quad (3)$$

where,  $\Delta q_{(001)LCL}$  is the broadening due to the finite LCL and  $\alpha_{tilt} \cdot q$  is the broadening due to the finite angle between the mosaic blocks. In our case where the instrumental broadening is of the order of 20 arc secs and the measured widths are of the order of 300 arc secs, the instrumental broadening effects have been neglected. However, this is strictly not the case in all the samples. The  $\omega$  - scans have a pseudo-Voigt line profile that is given by the equation:

$$y = y_o + A \left[ f \frac{(2w/\pi)}{4(x-x_c)^2 + w^2} + (1-f) \frac{\sqrt{4 \ln 2}}{\sqrt{\pi} w} e^{-\frac{4 \ln 2}{w^2}(x-x_c)^2} \right] \quad (4)$$

where,  $y_o$  is a constant,  $A$  is the amplitude,  $f$  is the fraction of Lorentzian component in the pseudo-Voigt profile ( $0 < f < 1$ ),  $w$  is the width of the curve, and  $x_c$  is the peak position. A perfect Lorentzian curve is given by  $f = 1$  and a perfect Gaussian is given by  $f = 0$ .

The addition of two pseudo-Voigt profiles with widths  $W_1$  and  $W_2$  gives a pseudo-Voigt profile with width  $W$ , given by the relation:

$$W^n = W_1^n + W_2^n \quad (5)$$

where,  $n = 1 + (1 - f)^2$  [12]. For a pseudo-Voigt profile,  $1 < n < 2$ .

According to the conventional analysis of the  $\omega$  - scans by W-H plots (Conventionally, the above method has been applied for a set of planes parallel to the sample surface, namely (002), (004) and (006)), the contributions due to the finite lateral size and the tilt are added. The tilt contribution is  $q$  dependant (proportional to  $q$ ) and the lateral size contribution is independent of  $q$ . The addition of these two factors for the case of a pseudo-Voigt profile can be written as:

$$\left(\Delta q_{obs}(\omega)\right)^n = \left(\Delta q_{(001)LCL}\right)^n + (\alpha_{tilt} \cdot q)^n \quad (6)$$

where,  $\Delta q_{obs}(\omega)$  is the total broadening of the  $\omega$  - scan peak in the  $q$  - space,  $\Delta q_{(001)LCL}$  is the contribution of the broadening due to finite LCL and  $\alpha_{tilt}$  is the tilt between the mosaic blocks in the film.

This analysis is however expected to fail in the presence of APDs in the films. The presence of APDs broaden the selective reflections namely (002) and (006) thereby making the equation 6 unusable. Further, in zinc-blende system, (006) is a very weak reflection, which makes the determination of the width highly erroneous.

To avoid this problem, a different set of parallel planes whose reciprocal lattice vector is inclined by some angle with the surface normal, have been used for the analysis. The (111), (333) and (444) reflections, which make an angle ( $\psi$ ) of  $54.73^\circ$  with the plane parallel to the surface, have been used. It is important that none of these planes are affected by APDs and all of them are allowed reflections that make the data quite strong and the FWHM can thus be determined without significant errors. The  $\omega$  - scans for these planes have been recorded in the skew-symmetry geometry to obtain the LCL and the angular broadening in the epilayers. The results related to this above modified analysis of the W-H plots are discussed in the next section.

A very important set of parameter that determines the quality of mosaic layer is the tilt and twist between the mosaic blocks of the epitaxial layer. Tilt and twist are out-of-plane and in-plane misorientation of the mosaic blocks in the epitaxial layer. To obtain the values of tilt and twist,  $\omega$  - scans are recorded for the planes whose angle of inclination with the substrate normal varies from  $0^\circ$  to  $90^\circ$  [12]. The width of x-ray peak obtained by  $\omega$  - scan for plane for which  $\psi = 0^\circ$  is tilt value and width for  $\psi = 90^\circ$  is the twist value. As the case of  $\psi = 90^\circ$  cannot be recorded in the reflecting geometry, an extrapolation scheme was first used by Srikant et al. [12]. However, the effect of finite LCL is not considered, as all the films analyzed in Ref. [12], had relatively large LCLs. For the set of (1,1,1) planes, the  $\omega$  - scan broadening may be written as:

$$\left(\Delta q_{obs}(\omega)\right)^n = \left(\Delta q_{(ll)LCL}\right)^n + \left(\alpha(l,l,l) * q\right)^n \quad (7)$$

where,  $\alpha(1,1,1)$  is the broadening of the (1,1,1) reflection due to a combination of tilt and twist.  $\Delta q_{(ll)LCL}$  is the y-axis intercept of the W-H plot for  $\omega$  - scans using (111), (333) and (444) reflections. The contribution of LCL to be peak broadening is eliminated from the  $\omega$  - scan of all the skew-symmetric reflections. Thus the LCL corrected angular broadening  $\alpha(h, k, l)$ , for any (h, k, l) reflection in the skew-symmetric geometry may be written as:

$$\alpha(h, k, l) = \left[ \left( \frac{\Delta q_{obs}}{q} \right)^n - \left( \frac{\Delta q_{(ll)LCL}}{q} \right)^n \right]^{1/n} \quad (8)$$

After the correction for the LCL, the expression for the width as a function of  $\psi$  may be written as [3,18]:

$$\alpha(h, k, l)^n = \left(\alpha_{tilt} \cos \psi\right)^n + \left(\alpha_{twist} \sin \psi\right)^n \quad (9)$$

The GaAs layers (samples ‘‘a’’, ‘‘b’’ and ‘‘c’’) were deposited by Metal Organic Vapour Phase Epitaxy (MOVPE) (AIXTRON AIX200) on (001)

oriented Si substrates. The samples “a”, “b” and “c”, have been deposited using a two step growth technique with different V/III ratios. The buffer layers were grown at 450 °C and at 400 °C and the epilayers at 650 °C, 670 °C, and 690 °C respectively for samples “a”, “b” and “c”. The thickness of the samples were determined by a thickness profilometer model Alpha-step IQ (KLA Tencor make). We present a detailed HRXRD study for the above three epilayers. The analysis is very general and can be used for any III-V epilayer especially those that are highly lattice mismatched where the issues of tilt, twist and LCL are very important.

### 3. RESULTS AND DISCUSSION

Fig. 1 shows the intensity vs.  $q_x$  curves derived from  $\omega$  - scans using eqn. 1 and 2 for (002), (004) and (006) reflection of layer “a”. The pseudo-Voigt fitting of the curves using eqn. 4 are shown by the overlaying lines in the figure. The weak reflection (006) reflection is very noisy and the fitting is erroneous. The observation is similar for all the remaining samples.

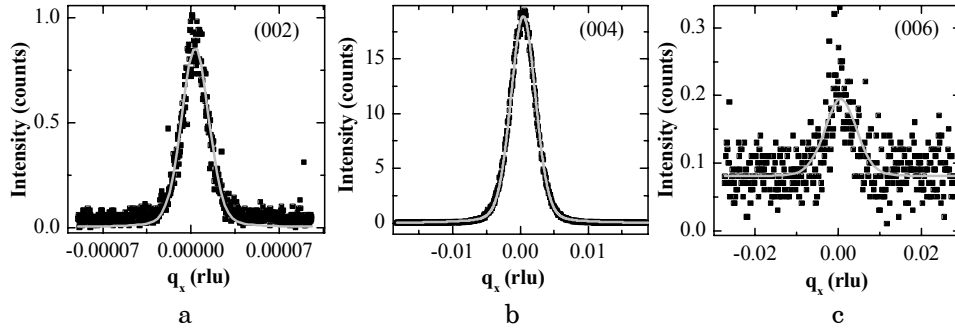


*Fig. 1 – The intensity vs.  $q_x$  curves for (002), (004) and (006) reflection of sample “a”. The fitting of the curve is shown by overlaying line*

Fig. 2a, b, and c shows the W-H plots using the  $\omega$  - scans for the layers “a”, “b” and “c” respectively using (002), (004) and (006) reflections. The value of “ $n$ ” used in the plots are determined from the pseudo-Voigt fitting of the  $\omega$  - scan profiles in the  $q$  - space using equations 1, 2 and 4. One finds that for all the layers, straight line fits, as expected from W-H plots are not obtained (Fig. 2a-c). This observation is attributed to two reasons. First, the values of the width of the (006) reflection, which is a forbidden reflection for zinc-blende structure, may be erroneous due to its very small intensity. Secondly, it may be noted that (002) and (006) reflections, are selectively broadened by the presence of APDs in the GaAs/Si samples i.e. epilayers “a”, “b” and “c”, thereby making the straight line fitting of the W-H plots impossible.

We have also made W-H plots using the  $\omega$  - scans of the (111), (333) and (444) reflections in the skew-symmetric geometry, from the epilayers “a”, “b” and “c” in Fig. 3a-c respectively. We find that straight-line fits are obtained in all the cases thereby enabling the possibly of using this analysis for this set of reflections. The value of the LCL and  $\alpha(1, 1, 1)$  for the films determined from the straight line fitting (also shown in Fig. 3a-c) is given

in Table 1. Thus we find that the choice of the diffraction planes in this case is extremely important and LCL values can only be determined in these films using the set of (1, 1, 1) planes.  $\alpha(1, 1, 1)$  values determined from these plots are a combination of tilt and twist in the layers and thus need to be analyzed further based on the procedure mentioned in the previous section.

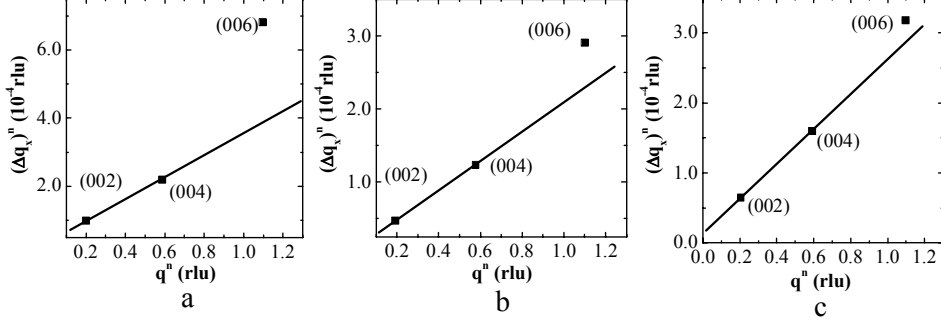


**Fig. 2** – *W-H plots for samples “a”, “b” and “c” using the (002), (004) and (006) reflections for the  $\omega$ -scan widths. The straight line is used to guide the reader’s eye*

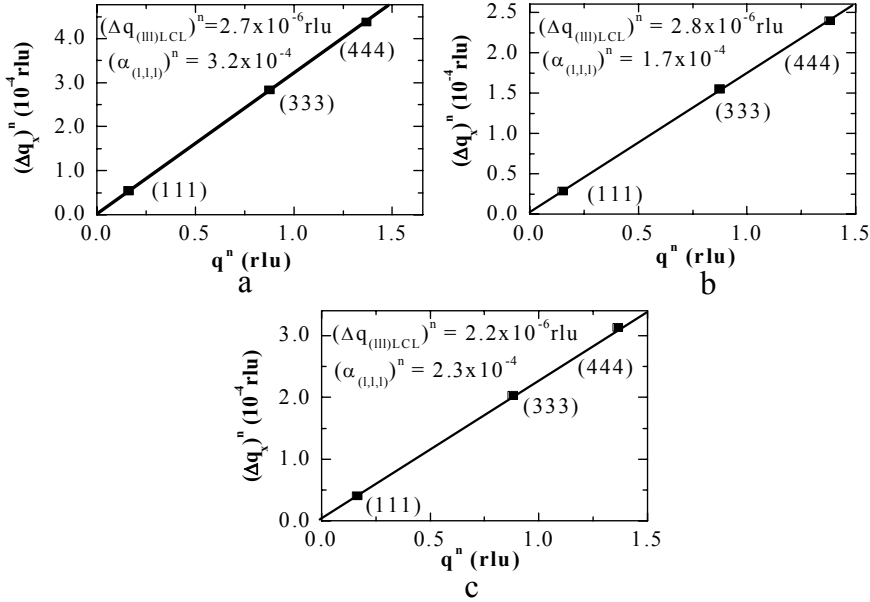


**Fig. 3** – *W-H plots for samples “a”, “b” and “c” using the (111), (333) and (444) reflections for the  $\omega$ -scan widths. The straight line shows the linear fitting of the points*

We estimate the tilt (out-of-plane misorientation of the blocks) and the twist (in-plane misorientation of the blocks) by making a series of reflections in the skew-symmetric geometry and plotting the width of these reflections as a function of  $\psi$ . The y axis ( $\omega$ -scan width) shown in Fig. 4, is equivalent to  $\Delta q_{obs}/q$  of eqn. 8. This is strictly true only for small  $\omega$  widths, which is

almost always the case with epitaxial films. These results are shown in Fig. 4a-c for the epilayers “a”, “b” and “c” respectively. The widths without the finite length corrections are shown in the inset of each figure. It is clear that the correction due to the finite length effects is mandatory and the data after the correction due to the finite lengths is seen to fit a monotonic line as expected from Eqn. 9. The fits to Eqn. 9 for all the films are shown in Fig 4a-c. The values of the tilt and twist are shown in the Table 1.

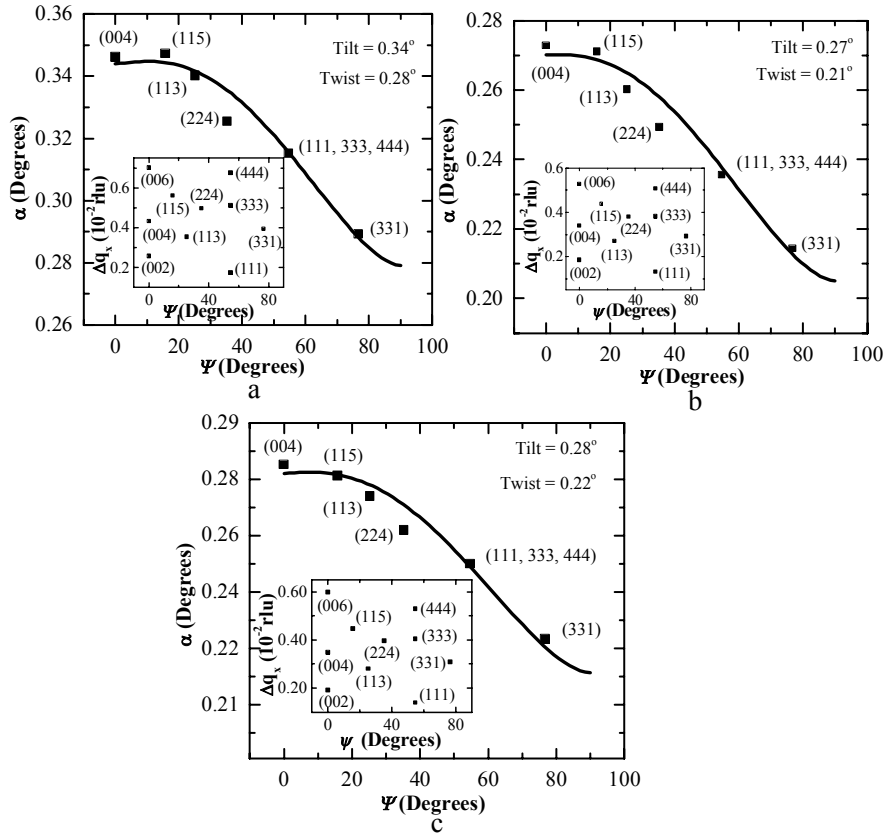


**Fig. 4** – Widths of  $\omega$ -scan data recorded in the skew-symmetric geometry corrected for the finite coherence lengths for the planes shown as a function of  $\psi$ . The data for the samples “a”, “b” and “c” are shown. Inset shows widths of  $\omega$ -scan data recorded in the skew-symmetric geometry for the planes shown in the inset as a function of  $\psi$ . The data for the samples “a”, “b” and “c” are shown

The tilt and twist values obtained for the films are directly related to the dislocation density of the films. This method has been the standard method for the determination of the dislocation density for III-Nitride epilayers where the systems are in almost all the cases grown on highly mismatched substrates. However for the case of III-V systems, almost all the work has been carried out on matched or nearly matched systems and thus there issues of tilt and twist between the mosaic blocks do not arise. However there are a few systems where this issue is important like the ones studied

in this work namely: GaAs/Si. The most common type of dislocation present in these systems are the ones that have a Burger's vector  $b = a/2 (0, 1, 1)$  and line of dislocation along:  $(1, -1, 0)$  direction, commonly referred to as the  $60^\circ$  dislocation. These are mixed dislocations that give rise to both tilt and twist in the epilayers. The details of the effects of the dislocations, their contribution to the tilt and twist and their relation to the measured TEM data will be a subject of a future work.

**Table 1** – The results obtained for the various epilayers “a”, “b and “c”

Sample Name	Sample Thickness ( $\mu\text{m}$ )	LCL determined From W-H plots ( $\mu\text{m}$ )	Tilt Determined from W-H plots (Degrees)	Twist Determined from W-H plots (Degrees)
a	0.31	0.40	0.34	0.28
b	0.31	0.31	0.28	0.22
c	0.33	0.51	0.27	0.21

#### 4. CONCLUSION

Standard W-H Analysis using (001) reflections ( $l = 2, 4, 6$ ) cannot be used with ease for the zinc-blende systems due to APDs and/or weak reflections. A modified W-H Analysis is presented in this work that can be used for a zinc-blende system. This approach is specifically applicable for the cases, where the films have APDs and/or some of the reflections in the W-H plot are not allowed and hence very weak. The LCL and the angular broadening of the mosaic blocks are determined from the W-H plots. The tilt and twist between the mosaic blocks in the epilayers is also obtained after correcting for the LCL.

The authors thank Dr. T.K. Sharma and Mr. S.D. Singh for help in the planning and growth of the samples, Dr. M.P. Joshi and Dr. Rajmohan for the thickness measurements and Dr. S.M. Oak for helpful discussions, encouragement and support. The authors also thank Mr. U.K. Ghosh and Mr. A. Khakha for their help during the growth of the samples.

#### REFERENCES

1. R. Chierchia, T. Buttcher, H. Heinke, S. Einfeldt, S. Figge, D. Hommel, *J. Appl. Phys.* **93**, 8918 (2003).
2. M.E Vickers, M.J Kappers, R Datta, C McAleese, T.M Smeeton, F.D.G Rayment, C.J Humphreys, *J. Phys. D: Appl. Phys.* **38**, A99 (2005).
3. S.R. Lee, A.M. West, A.A. Allerman, K.E. Waldrip, D.M. Follstaedt, P.P. Proventio, D.D. Koleske, C.R. Abernathy, *Appl. Phys. Lett.* **86**, 241904 (2005).
4. T. Ganguli, A. Kadir, M. Gokhale, R. Kumar, A.P. Shah, B.M. Arora, A. Bhattacharya, *J. Cryst. Growth* **310**, 4942 (2008).
5. X.L. Zhu, L.W. Guo, N.S. Yu, J.F. Yan, M.Z. Peng, J. Zhang, H.Q. Jia, H. Chen, J.M. Zhou, *J. Cryst. Growth* **306**, 292 (2007).
6. S. Singh, R. Kumar, T. Ganguli, R.S. Srinivasa, S.S. Major, *J. Cryst. Growth* **310**, 4640 (2008).
7. G.K. Williamson, W.H. Hall, *Acta Metall.* **1**, 22 (1953).



8. B.S. Yadav, S. Singh, T. Ganguli, R. Kumar, S.S. Major, R.S. Srinivasa, *Thin Solid Films* **517**, 488 (2008).
9. S. Singh, T. Ganguli, R. Kumar, R.S. Srinivasa, S.S. Major, *Thin Solid Films* **517**, 661 (2008).
10. D.A. Neumann, H. Zabel, R. Fischer, H. Morkoz, *J. Appl. Phys.* **61**, 1023 (1987).
11. B.E. Warren, *X-ray diffraction* (New York, Courier Dover Publications: 1990).
12. V. Srikant, J.S. Speck D.R. Clarke, *J. Appl. Phys.* **82**, 4286 (1997).
13. T. Metzger, R. Hübler, E. Born, O. Ambacher, M. Stutzmann, R. Stommer, M. Schuster, H. Gobel, S. Christiansen, M. Albrecht, H.P. Strunk, *Philos. Mag. A* **77**, 1013 (1998).
14. V.K. Dixit, T. Ganguli, T.K. Sharma, S.D. Singh, R. Kumar, S. Porwal, P. Tiwari, A. Ingale, S.M. Oak, *J. Cryst. Growth* **310**, 3428 (2008).
15. S.H. Vajargah, M Couillard, Y. Shao, S. Tavakoli, R. Kleiman, J. Preston, G.A. Botton, *Microsc. Microanal.* **16**, 1338 (2010).
16. K. Li, J. Lin, A.T.S. Wee, K.L. Tan, Z.C. Feng, J.B. Webb, *Appl. Surf. Sci.* **99**, 59 (1996).
17. H. Yamaguchi, K. Kanisawa, S. Miyashita, Y. Hirayama, *Physica E* **23**, 285 (2004).
18. M.A. Moram, M.E. Vickers, *Rep. Prog. Phys.* **72**, 036502 (2009).
19. V.K. Dixit, T. Ganguli, T.K. Sharma, R. Kumar, S. Porwal, V. Shukla, A. Ingale, P. Tiwari, A.K. Nath, *J. Cryst. Growth* **293**, 5 (2006).
20. Z. Zhaochun, Q. Xiaoyan, C. Deliang, K. Xianggui, H. Baibiao, J. Minhua, *Mater. Sci. Eng. B* **77**, 24 (2000).